Discrete polytopal complexes for fluid mechanics, electromagnetism and solid mechanics

Jérôme Droniou

IMAG, CNRS & University of Montpellier, France,
School of Mathematics, Monash University, Australia

https://imag.umontpellier.fr/~droniou/

GAMNI 2025

IMAG INSTITUT MONTPELLIERAIN ALEXANDER GROTHENDIECK
cnrs
NEMESIS New generation methods for numerical simulations
Funded by the European Union
erc European Research Council Established by the European Commission

Outline

1. Some PDE models of interest
   - Stokes I
   - Stokes II
   - Navier–Stokes
   - Magnetostatics
2. De Rham complex
3. Discrete De Rham (DDR) complex
4. Applications to the models of interest

Slides

Outline

1. Some PDE models of interest
   - Stokes I
   - Stokes II
   - Navier–Stokes
   - Magnetostatics
2. De Rham complex
3. Discrete De Rham (DDR) complex
4. Applications to the models of interest

Slides

Stokes equations: standard formulation

Ω domain, $\nu > 0$ and $\boldsymbol{f} \in \boldsymbol{L}^2(\Omega)$.

- Strong form: Find $\boldsymbol{u} : \Omega \to \mathbb{R}^3$ and $p : \Omega \to \mathbb{R}$ s.t. $\int_\Omega p = 0$ and

$$\begin{aligned} -\nu \boldsymbol{\Delta u} + \mathbf{grad}\, p &= \boldsymbol{f} && \text{in } \Omega, && \text{(momentum conservation)} \\ \operatorname{div} \boldsymbol{u} &= 0 && \text{in } \Omega, && \text{(mass conservation)} \\ \boldsymbol{u} &= \boldsymbol{0} && \text{on } \partial\Omega, && \text{(boundary condition)} \end{aligned}$$

- Weak form: Find $(\boldsymbol{u}, p) \in H_0^1(\Omega)^d \times L^2(\Omega)$ s.t. $\int_\Omega p = 0$ and

$$\begin{aligned} \nu(\mathbf{grad}\, \boldsymbol{u}, \mathbf{grad}\, \boldsymbol{v})_{L^2} - (p, \operatorname{div} \boldsymbol{v})_{L^2} &= (\boldsymbol{f}, \boldsymbol{v})_{L^2} && \forall \boldsymbol{v} \in H_0^1(\Omega), \\ (\operatorname{div} \boldsymbol{u}, q)_{L^2} &= 0 && \forall q \in L^2(\Omega) \end{aligned}$$

Stokes equations: standard formulation

Ω domain, $\nu > 0$ and $\boldsymbol{f} \in \boldsymbol{L}^2(\Omega)$.

- Strong form: Find $\boldsymbol{u} : \Omega \to \mathbb{R}^3$ and $p : \Omega \to \mathbb{R}$ s.t. $\int_\Omega p = 0$ and

$$\begin{aligned} -\nu \boldsymbol{\Delta u} + \mathbf{grad}\, p &= \boldsymbol{f} && \text{in } \Omega, && \text{(momentum conservation)} \\ \operatorname{div} \boldsymbol{u} &= 0 && \text{in } \Omega, && \text{(mass conservation)} \\ \boldsymbol{u} &= \boldsymbol{0} && \text{on } \partial\Omega, && \text{(boundary condition)} \end{aligned}$$

- Weak form: Find $(\boldsymbol{u}, p) \in H^1_0(\Omega)^d \times L^2(\Omega)$ s.t. $\int_\Omega p = 0$ and

$$\begin{aligned} \nu(\mathbf{grad}\, \boldsymbol{u}, \mathbf{grad}\, \boldsymbol{v})_{L^2} - (p, \operatorname{div} \boldsymbol{v})_{L^2} &= (\boldsymbol{f}, \boldsymbol{v})_{L^2} && \forall \boldsymbol{v} \in H^1_0(\Omega), \\ (\operatorname{div} \boldsymbol{u}, q)_{L^2} &= 0 && \forall q \in L^2(\Omega) \end{aligned}$$

- A priori estimates require: ([1])

  - Poincaré inequality: $\|\cdot\|_{L^2} \lesssim \|\mathbf{grad} \cdot\|_{L^2}$ on $H^1_0(\Omega)$,
  - inf-sup: $\sup_{\boldsymbol{v} \in H^1_0} \frac{(p, \operatorname{div} \boldsymbol{v})_{L^2}}{\|\boldsymbol{v}\|_{H^1_0}} \geq C\|p\|_{L^2}$, i.e. $\operatorname{Im} \operatorname{div} = L^2(\Omega)$.

[1] $a \lesssim b$ means $a \leq Cb$ with C independent of a, b.

Outline

1. Some PDE models of interest
   - Stokes I
   - Stokes II
   - Navier–Stokes
   - Magnetostatics
2. De Rham complex
3. Discrete De Rham (DDR) complex
4. Applications to the models of interest

Slides

Stokes in curl-curl formulation: weak form

- Strong form:

$$\begin{aligned}
\overbrace{\nu(\mathbf{curl}\,\mathbf{curl}\,\boldsymbol{u} - \mathbf{grad}\,\mathrm{div}\,\boldsymbol{u})}^{-\nu\boldsymbol{\Delta}\boldsymbol{u}} + \mathbf{grad}\,p = \boldsymbol{f} \quad & \text{in } \Omega, && \text{(momentum cons.)}\\
\mathrm{div}\,\boldsymbol{u} = 0 \quad & \text{in } \Omega, && \text{(mass conservation)}\\
\mathbf{curl}\,\boldsymbol{u} \times \mathbf{n} = \mathbf{0} \text{ and } \boldsymbol{u}\cdot\mathbf{n} = 0 \quad & \text{on } \partial\Omega, && \text{(boundary conditions)}\\
\textstyle\int_\Omega p = 0 \quad &
\end{aligned}$$

- Weak form: Find $(\boldsymbol{u}, p) \in \boldsymbol{H}(\mathbf{curl};\Omega) \times H^1(\Omega)$ s.t. $\int_\Omega p = 0$ and

$$\begin{aligned}
\nu(\mathbf{curl}\,\boldsymbol{u}, \mathbf{curl}\,\boldsymbol{v})_{L^2} + (\mathbf{grad}\,p, \boldsymbol{v})_{L^2} &= (\boldsymbol{f}, \boldsymbol{v})_{L^2} && \forall \boldsymbol{v} \in \boldsymbol{H}(\mathbf{curl};\Omega),\\
-(\boldsymbol{u}, \mathbf{grad}\,q)_{L^2} &= 0 && \forall q \in H^1(\Omega),
\end{aligned}$$

where

$$\boldsymbol{H}(\mathbf{curl};\Omega) \coloneqq \left\{\boldsymbol{v} \in \boldsymbol{L}^2(\Omega)\ :\ \mathbf{curl}\,\boldsymbol{v} \in \boldsymbol{L}^2(\Omega)\right\}.$$

Stokes equations in curl-curl formulation: stability

$$\begin{aligned} \nu(\mathbf{curl}\,\boldsymbol{u}, \mathbf{curl}\,\boldsymbol{v})_{L^2} + (\mathbf{grad}\,p, \boldsymbol{v})_{L^2} &= (\boldsymbol{f}, \boldsymbol{v})_{L^2} \quad && \forall \boldsymbol{v} \in \boldsymbol{H}(\mathbf{curl};\Omega), \\ -(\boldsymbol{u}, \mathbf{grad}\,q)_{L^2} &= 0 && \forall q \in H^1(\Omega) \end{aligned}$$

- Make $\boldsymbol{v} = \mathbf{grad}\,p$ to get $\|\mathbf{grad}\,p\|_{L^2} \leq \|\boldsymbol{f}\|_{L^2}$ since $\mathbf{curl}\,\mathbf{grad} = 0$.
- Make $(\boldsymbol{v}, q) = (\boldsymbol{u}, p)$:

$$\nu\|\mathbf{curl}\,\boldsymbol{u}\|_{L^2}^2 \leq \|\boldsymbol{f}\|_{L^2}\|\boldsymbol{u}\|_{L^2}.$$

Stokes equations in curl-curl formulation: stability

$$\nu(\mathbf{curl}\,\boldsymbol{u}, \mathbf{curl}\,\boldsymbol{v})_{L^2} + (\mathbf{grad}\,p, \boldsymbol{v})_{L^2} = (\boldsymbol{f}, \boldsymbol{v})_{L^2} \quad \forall \boldsymbol{v} \in \boldsymbol{H}(\mathbf{curl};\Omega),$$
$$-(\boldsymbol{u}, \mathbf{grad}\,q)_{L^2} = 0 \quad \forall q \in H^1(\Omega)$$

- Make $\boldsymbol{v} = \mathbf{grad}\,p$ to get $\|\mathbf{grad}\,p\|_{L^2} \leq \|\boldsymbol{f}\|_{L^2}$ since $\mathbf{curl}\,\mathbf{grad} = 0$.
- Make $(\boldsymbol{v}, q) = (\boldsymbol{u}, p)$:

$$\nu\|\mathbf{curl}\,\boldsymbol{u}\|_{L^2}^2 \leq \|\boldsymbol{f}\|_{L^2}\|\boldsymbol{u}\|_{L^2}.$$

- If Ω "is nice",

$$\mathrm{Im}\,\mathbf{grad} = \mathrm{Ker}\,\mathbf{curl}.$$

The incompressibility then gives $\boldsymbol{u} \in (\mathrm{Im}\,\mathbf{grad})^\perp = (\mathrm{Ker}\,\mathbf{curl})^\perp$ and the

Poincaré inequality: $\|\cdot\|_{L^2} \lesssim \|\mathbf{curl}\cdot\|_{L^2}$ on $(\mathrm{Ker}\,\mathbf{curl})^\perp$

yields

$$\|\boldsymbol{u}\|_{L^2} \lesssim \|\mathbf{curl}\,\boldsymbol{u}\|_{L^2}.$$

Outline

Slides

Navier-Stokes equations

- Additional convective term:

$$\operatorname{div}(\boldsymbol{u} \otimes \boldsymbol{u}) = (\operatorname{div} \boldsymbol{u})\boldsymbol{u} + (\mathbf{curl}\, \boldsymbol{u}) \times \boldsymbol{u} + \frac{1}{2} \mathbf{grad}\, |\boldsymbol{u}|^2.$$

so

$$-\nu \Delta \boldsymbol{u} + (\boldsymbol{u} \cdot \nabla)\boldsymbol{u} + \mathbf{grad}\, p = \nu\, \mathbf{curl}\, \mathbf{curl}\, \boldsymbol{u} + \underbrace{(\mathbf{curl}\, \boldsymbol{u}) \times \boldsymbol{u}}_{\text{additional term}} + \mathbf{grad} \underbrace{\left(p + \frac{1}{2}|\boldsymbol{u}|^2\right)}_{\text{new pressure } p'}$$

- Additional term in weak formulation

$$\int_\Omega [(\mathbf{curl}\, \boldsymbol{u}) \times \boldsymbol{u}] \cdot \boldsymbol{v}.$$

It vanishes for $\boldsymbol{v} = \boldsymbol{u}$.

Outline

1 Some PDE models of interest
- Stokes I
- Stokes II
- Navier–Stokes
- Magnetostatics

2 De Rham complex

3 Discrete De Rham (DDR) complex

4 Applications to the models of interest

Slides

Magnetostatics: weak formulation

- Strong form: For $\mu > 0$ and $\boldsymbol{J} \in \mathbf{curl}\, \boldsymbol{H}(\mathbf{curl};\Omega)$, the magnetostatics problem reads:

  Find the magnetic field $\boldsymbol{H} : \Omega \to \mathbb{R}^3$ and vector potential $\boldsymbol{A} : \Omega \to \mathbb{R}^3$ s.t.

$$\begin{aligned}
\mu \boldsymbol{H} - \mathbf{curl}\, \boldsymbol{A} &= \mathbf{0} && \text{in } \Omega, && \text{(vector potential)}\\
\mathbf{curl}\, \boldsymbol{H} &= \boldsymbol{J} && \text{in } \Omega, && \text{(Ampère's law)}\\
\operatorname{div} \boldsymbol{A} &= 0 && \text{in } \Omega, && \text{(Coulomb's gauge)}\\
\boldsymbol{A} \times \mathbf{n} &= \mathbf{0} && \text{on } \partial\Omega && \text{(boundary condition)}
\end{aligned}$$

- Weak form: Find $(\boldsymbol{H}, \boldsymbol{A}) \in \boldsymbol{H}(\mathbf{curl};\Omega) \times \boldsymbol{H}(\operatorname{div};\Omega)$ s.t.

$$\begin{aligned}
\int_\Omega \mu \boldsymbol{H} \cdot \boldsymbol{\tau} - \int_\Omega \boldsymbol{A} \cdot \mathbf{curl}\, \boldsymbol{\tau} &= 0 && \forall \boldsymbol{\tau} \in \boldsymbol{H}(\mathbf{curl};\Omega),\\
\int_\Omega \mathbf{curl}\, \boldsymbol{H} \cdot \boldsymbol{v} + \int_\Omega \operatorname{div} \boldsymbol{A} \operatorname{div} \boldsymbol{v} &= \int_\Omega \boldsymbol{J} \cdot \boldsymbol{v} && \forall \boldsymbol{v} \in \boldsymbol{H}(\operatorname{div};\Omega).
\end{aligned}$$

Magnetostatics: requirements for stability

Relations images/kernels:

$$\operatorname{Im}\mathbf{curl} = \operatorname{Ker}\operatorname{div}\,,$$
$$\operatorname{Im}\operatorname{div} = L^2(\Omega).$$

Poincaré inequalities:

$$\|\cdot\|_{L^2} \leq C\|\operatorname{div}\cdot\|_{L^2} \quad \text{on } (\operatorname{Ker}\operatorname{div})^\perp$$
$$\|\cdot\|_{L^2} \leq C\|\mathbf{curl}\cdot\|_{L^2} \quad \text{on } (\operatorname{Ker}\mathbf{curl})^\perp.$$

Outline

1 Some PDE models of interest
- Stokes I
- Stokes II
- Navier–Stokes
- Magnetostatics

2 De Rham complex

3 Discrete De Rham (DDR) complex

4 Applications to the models of interest

Slides

De Rham complex

$$H^1(\Omega) \xrightarrow{\mathbf{grad}} \boldsymbol{H}(\mathbf{curl};\Omega) \xrightarrow{\mathbf{curl}} \boldsymbol{H}(\mathrm{div};\Omega) \xrightarrow{\mathrm{div}} L^2(\Omega) \xrightarrow{0} \{0\}$$

- Complex: image of an operator included in kernel of the next one.

  That is, the composition of two subsequent operators vanishes.

De Rham complex

$$H^1(\Omega) \xrightarrow{\mathbf{grad}} \boldsymbol{H}(\mathbf{curl};\Omega) \xrightarrow{\mathbf{curl}} \boldsymbol{H}(\mathrm{div};\Omega) \xrightarrow{\mathrm{div}} L^2(\Omega) \xrightarrow{0} \{0\}$$

- Complex: image of an operator included in kernel of the next one.
- Depending on the topology of Ω, some inclusions can be equalities:

$$\text{no "tunnels"} \implies \mathrm{Im}\,\mathbf{grad} = \mathrm{Ker}\,\mathbf{curl} \quad \text{(Stokes in curl-curl)}$$

$$\text{no "voids"} \implies \mathrm{Im}\,\mathbf{curl} = \mathrm{Ker}\,\mathrm{div} \quad \text{(magnetostatics)}$$

$$\mathrm{Im}\,\mathrm{div} = L^2(\Omega) \quad \text{(magnetostatics, standard Stokes)}$$

De Rham complex

$$H^1(\Omega) \xrightarrow{\mathbf{grad}} \boldsymbol{H}(\mathbf{curl};\Omega) \xrightarrow{\mathbf{curl}} \boldsymbol{H}(\mathrm{div};\Omega) \xrightarrow{\mathrm{div}} L^2(\Omega) \xrightarrow{0} \{0\}$$

- Complex: image of an operator included in kernel of the next one.
- Depending on the topology of Ω, some inclusions can be equalities:

$$\text{no "tunnels"} \implies \mathrm{Im}\,\mathbf{grad} = \mathrm{Ker}\,\mathbf{curl} \quad \text{(Stokes in curl-curl)}$$
$$\text{no "voids"} \implies \mathrm{Im}\,\mathbf{curl} = \mathrm{Ker}\,\mathrm{div} \quad \text{(magnetostatics)}$$
$$\mathrm{Im}\,\mathrm{div} = L^2(\Omega) \quad \text{(magnetostatics, standard Stokes)}$$

- If Ω has a non-trivial topology, the de Rham's cohomology characterizes

$$\mathrm{Ker}\,\mathbf{curl}\,/\,\mathrm{Im}\,\mathbf{grad} \quad \text{and} \quad \mathrm{Ker}\,\mathrm{div}\,/\,\mathrm{Im}\,\mathbf{curl}$$

Reproducing these properties at the discrete level is key for stable schemes.

Outline

Slides

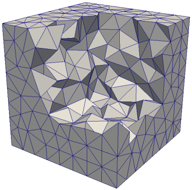

$\mathcal{T}_h = \{T\}$ conforming tetrahedral/hexahedral mesh.

- Define local polynomial spaces on each element, and glue them together to form a sub-complex of the de Rham complex:

$$\begin{array}{ccccccc} V_h^0 & \xrightarrow{\mathbf{grad}} & V_h^1 & \xrightarrow{\mathbf{curl}} & V_h^2 & \xrightarrow{\mathrm{div}} & V_h^3 \\ \downarrow & & \downarrow & & \downarrow & & \downarrow \\ H^1(\Omega) & \xrightarrow{\mathbf{grad}} & \boldsymbol{H}(\mathbf{curl};\Omega) & \xrightarrow{\mathbf{curl}} & \boldsymbol{H}(\mathrm{div};\Omega) & \xrightarrow{\mathrm{div}} & L^2(\Omega) \end{array}$$

Example: conforming $\mathcal{P}^k$–Nédélec–Raviart-Thomas spaces [Arnold, 2018].

- **Gluing only works on special meshes!**

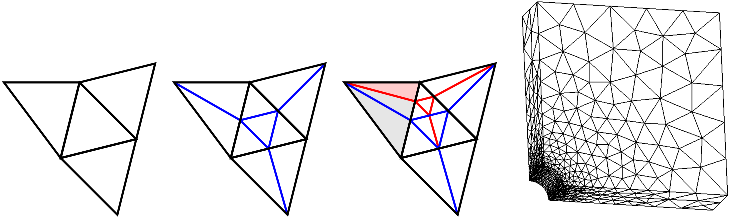

- Approach limited to conforming meshes with standard elements
  - ⟹ local refinement requires to trade mesh size for mesh quality
  - ⟹ complex geometries may require a large number of elements
  - ⟹ the element shape cannot be adapted to the solution
- Need for (global) basis functions
  - ⟹ significant increase of DOFs on hexahedral elements

Benefits of polytopal meshes I

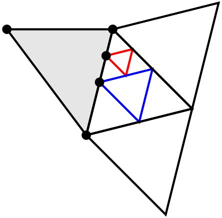

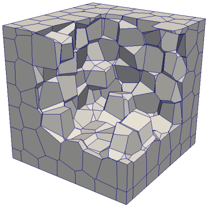

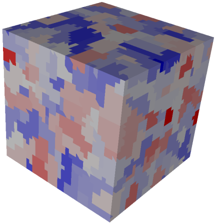

- Local refinement (to capture geometry or solution features) is seamless, and can preserve mesh regularity.
- Agglomerated elements are also easy to handle (and useful, e.g., in multi-grid methods).
- Even on standard meshes, high-level approach can lead to leaner methods (fewer DOFs).

Benefits of polytopal meshes II

Discrete space	$k = 0$	$k = 1$	$k = 2$
$H^1(T)$	4 ♢ 4	10 ♢ 10	20 ♢ 20
$\boldsymbol{H}(\mathbf{curl}; T)$	6 ♢ 6	23 ♢ 20	53 ♢ 45
$\boldsymbol{H}(\mathrm{div}; T)$	4 ♢ 4	18 ♢ 15	44 ♢ 36
$L^2(T)$	1 ♢ 1	4 ♢ 4	10 ♢ 10

Table: Tetrahedron: SDDR polytopal complex ♢ RTN.

Discrete space	$k = 0$	$k = 1$	$k = 2$
$H^1(T)$	8 ♢ 8	20 ♢ 27	32 ♢ 64
$\boldsymbol{H}(\mathbf{curl}; T)$	12 ♢ 12	39 ♢ 54	77 ♢ 144
$\boldsymbol{H}(\mathrm{div}; T)$	6 ♢ 6	24 ♢ 36	56 ♢ 108
$L^2(T)$	1 ♢ 1	4 ♢ 8	10 ♢ 27

Table: Hexahedron: SDDR polytopal complex ♢ RTN.

[Di Pietro and Droniou, 2023c]

Building blocks of the Discrete De Rham complex

Refs.: [Di Pietro et al., 2020, Di Pietro and Droniou, 2023a]

- Hierarchical constructions: from lowest-dimensional mesh entity to higher-dimensional entities.

- Enhancement:
  - discrete differential operator first,
  - potential reconstruction using the discrete differential operator.

  (both polynomially consistent, both based on IBP formulas.)

- The definition of the spaces (DOFs) also guided by these IBP formulas.

Same guiding principles as the Hybrid High-Order (HHO) method [Di Pietro and Droniou, 2020].

Mesh notations

- Mesh $\mathcal{M}_h = (\mathcal{T}_h, \mathcal{F}_h, \mathcal{E}_h, \mathcal{V}_h)$ of elements/faces/edges/vertices, with intrinsic orientations (tangent, normal).
- $\omega_{TF} \in \{+1, -1\}$ such that $\omega_{TF}\mathbf{n}_F$ outer normal to T.
- $\omega_{FE} \in \{+1, -1\}$ such that $\omega_{FE}\mathbf{t}_E$ clockwise on F.

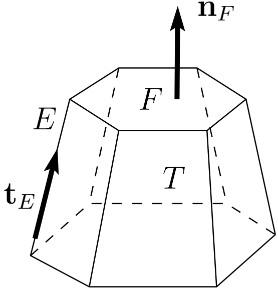

$\mathcal{P}^k$-consistent gradient
Edge E

- IBP is the starting point: if $q \in \mathcal{P}^{k+1}(E)$ then

$$\int_E q' r = -\int_E q \underbrace{r'}_{\in \mathcal{P}^{k-1}(E)} + q(\boldsymbol{x}_{V_2}) r(\boldsymbol{x}_{V_2}) - q(\boldsymbol{x}_{V_1}) r(\boldsymbol{x}_{V_1}) \qquad \forall r \in \mathcal{P}^k(E)$$

  with derivatives in the direction $\mathbf{t}_E$.

$\mathcal{P}^k$-consistent gradient

Edge E

- IBP is the starting point: if $q \in \mathcal{P}^{k+1}(E)$ then

$$\int_E q' r = -\int_E \pi_{r,E}^{k-1} q \underbrace{r'}_{\in \mathcal{P}^{k-1}(E)} + q(\boldsymbol{x}_{V_2}) r(\boldsymbol{x}_{V_2}) - q(\boldsymbol{x}_{V_1}) r(\boldsymbol{x}_{V_1}) \qquad \forall r \in \mathcal{P}^k(E)$$

  with $\pi_{r,E}^{k-1}$ the L^2-projection on $\mathcal{P}^{k-1}(E)$.

$\mathcal{P}^k$-consistent gradient
Edge E

- IBP is the starting point: if $q \in \mathcal{P}^{k+1}(E)$ then

$$\int_E q' r = -\int_E \pi_{r,E}^{k-1} q \underbrace{r'}_{\in \mathcal{P}^{k-1}(E)} + q(\boldsymbol{x}_{V_2}) r(\boldsymbol{x}_{V_2}) - q(\boldsymbol{x}_{V_1}) r(\boldsymbol{x}_{V_1}) \qquad \forall r \in \mathcal{P}^k(E)$$

- Space and interpolator:

$$\underline{X}_{\mathbf{grad},E}^k = \left\{ \underline{q}_E = (q_E, (q_V)_{V \in \mathcal{V}_E}) \,:\, q_E \in \mathcal{P}^{k-1}(E)\,,\ q_V \in \mathbb{R} \right\},$$

$$\underline{I}_{\mathbf{grad},E}^k q = (\pi_{r,E}^{k-1} q, (q(\boldsymbol{x}_V))_{V \in \mathcal{V}_E}) \qquad \forall q \in C(\overline{E}).$$

$\mathcal{P}^k$-consistent gradient

Edge E

- IBP is the starting point: if $q \in \mathcal{P}^{k+1}(E)$ then

$$\int_E q' r = -\int_E \pi^{k-1}_{r,E} q \underbrace{r'}_{\in \mathcal{P}^{k-1}(E)} + q(\boldsymbol{x}_{V_2}) r(\boldsymbol{x}_{V_2}) - q(\boldsymbol{x}_{V_1}) r(\boldsymbol{x}_{V_1}) \qquad \forall r \in \mathcal{P}^k(E)$$

- Space: $\underline{X}^k_{\mathbf{grad},E} = \left\{ \underline{q}_E = (q_E, (q_V)_{V \in \mathcal{V}_E}) \,:\, q_E \in \mathcal{P}^{k-1}(E)\,,\ q_V \in \mathbb{R} \right\}$.
- Edge gradient $G^k_E : \underline{X}^k_{\mathbf{grad},E} \to \mathcal{P}^k(E)$ s.t.

$$\int_E (G^k_E \underline{q}_E) r = -\int_E q_E r' + q_{V_2} r(\boldsymbol{x}_{V_2}) - q_{V_1} r(\boldsymbol{x}_{V_1}) \qquad \forall r \in \mathcal{P}^k(E).$$

- IBP is the starting point: if $q \in \mathcal{P}^{k+1}(E)$ then

$$\int_E q' r = -\int_E \pi_{r,E}^{k-1} q \underbrace{r'}_{\in \mathcal{P}^{k-1}(E)} + q(\boldsymbol{x}_{V_2}) r(\boldsymbol{x}_{V_2}) - q(\boldsymbol{x}_{V_1}) r(\boldsymbol{x}_{V_1}) \qquad \forall r \in \mathcal{P}^k(E)$$

- Space: $\underline{X}_{\mathbf{grad},E}^k = \left\{ \underline{q}_E = (q_E, (q_V)_{V \in \mathcal{V}_E}) \,:\, q_E \in \mathcal{P}^{k-1}(E)\,,\; q_V \in \mathbb{R} \right\}$.
- Edge gradient $G_E^k : \underline{X}_{\mathbf{grad},E}^k \to \mathcal{P}^k(E)$ s.t.

$$\int_E (G_E^k \underline{q}_E) r = -\int_E q_E r' + q_{V_2} r(\boldsymbol{x}_{V_2}) - q_{V_1} r(\boldsymbol{x}_{V_1}) \qquad \forall r \in \mathcal{P}^k(E).$$

- Potential reconstruction $\gamma_E^{k+1} : \underline{X}_{\mathbf{grad},E}^k \to \mathcal{P}^{k+1}(E)$ s.t.

$$\int_E (\gamma_E^{k+1} \underline{q}_E) z' = -\int_E (G_E^k \underline{q}_E) z + q_{V_2} z(\boldsymbol{x}_{V_2}) - q_{V_1} z(\boldsymbol{x}_{V_1}) \qquad \forall z \in \mathcal{P}^{k+2}(E).$$

(Works because $\frac{d}{dx} : \mathcal{P}^{k+2}(E)/\mathbb{R} \to \mathcal{P}^{k+2}(E)$ is an isomorphism.)

$\mathcal{P}^k$-consistent gradient
Face F

- IBP is the starting point: if $q \in \mathcal{P}^{k+1}(F)$,

$$\int_F (\mathbf{grad}_F\, q) \cdot \boldsymbol{v} = -\int_F q \underbrace{\mathrm{div}_F\, \boldsymbol{v}}_{\in \mathcal{P}^{k-1}(F)} + \sum_{E \in \mathcal{E}_F} \omega_{FE} \int_E q \boldsymbol{v} \cdot \mathbf{n}_{FE} \quad \forall \boldsymbol{v} \in \mathcal{P}^k(F)^2.$$

$\mathcal{P}^k$-consistent gradient

Face F

- IBP is the starting point: if $q \in \mathcal{P}^{k+1}(F)$,

$$\int_F (\mathbf{grad}_F\, q)\cdot\boldsymbol{v} = -\int_F \pi_{r,F}^{k-1} q \underbrace{\operatorname{div}_F \boldsymbol{v}}_{\in\mathcal{P}^{k-1}(F)} + \sum_{E\in\mathcal{E}_F} \omega_{FE} \int_E q\boldsymbol{v}\cdot\mathbf{n}_{FE} \quad \forall \boldsymbol{v} \in \mathcal{P}^k(F)^2.$$

$\mathcal{P}^k$-consistent gradient

Face F

- IBP is the starting point: if $q \in \mathcal{P}^{k+1}(F)$,

$$\int_F (\mathbf{grad}_F\, q)\cdot\boldsymbol{v} = -\int_F \pi_{r,F}^{k-1} q \underbrace{\operatorname{div}_F \boldsymbol{v}}_{\in\mathcal{P}^{k-1}(F)} + \sum_{E\in\mathcal{E}_F} \omega_{FE} \int_E q\boldsymbol{v}\cdot\mathbf{n}_{FE} \quad \forall \boldsymbol{v}\in\mathcal{P}^k(F)^2.$$

- Space and interpolator:

$$\underline{X}_{\mathbf{grad},F}^k = \Big\{ \underline{q}_F = (q_F, (q_E)_{E\in\mathcal{E}_F}, (q_V)_{V\in\mathcal{V}_F}) \,:\, q_F \in \mathcal{P}^{k-1}(F),\ q_E\in\mathcal{P}^{k-1}(E),\ q_V\in\mathbb{R} \Big\},$$

$$\underline{I}_{\mathbf{grad},F}^k q = (\pi_{r,F}^{k-1} q, (\pi_{r,E}^{k-1} q_{|E})_{E\in\mathcal{E}_F}, (q(\boldsymbol{x}_V))_{V\in\mathcal{V}_F}) \qquad \forall q\in C(\overline{F}).$$

$\mathcal{P}^k$-consistent gradient

Face F

- IBP is the starting point: if $q \in \mathcal{P}^{k+1}(F)$,

$$\int_F (\mathbf{grad}_F\, q)\cdot\boldsymbol{v} = -\int_F \pi^{k-1}_{r,F} q \underbrace{\operatorname{div}_F \boldsymbol{v}}_{\in\mathcal{P}^{k-1}(F)} + \sum_{E\in\mathcal{E}_F} \omega_{FE} \int_E q\boldsymbol{v}\cdot\mathbf{n}_{FE} \quad \forall \boldsymbol{v}\in\mathcal{P}^k(F)^2.$$

- Space :

$$\underline{X}^k_{\mathbf{grad},F} = \Big\{ \underline{q}_F = (q_F, (q_E)_{E\in\mathcal{E}_F}, (q_V)_{V\in\mathcal{V}_F}) \ : \ q_F \in \mathcal{P}^{k-1}(F),\ q_E \in \mathcal{P}^{k-1}(E),\ q_V \in \mathbb{R} \Big\},$$

- Face gradient $\mathbf{G}^k_F : \underline{X}^k_{\mathbf{grad},F} \to \mathcal{P}^k(F)^2$ s.t.

$$\int_F (\mathbf{G}^k_F \underline{q}_F)\cdot\boldsymbol{v} = -\int_F q_F \operatorname{div}_F \boldsymbol{v} + \sum_{E\in\mathcal{E}_F} \omega_{FE} \int_E (\gamma^{k+1}_E \underline{q}_E)\boldsymbol{v}\cdot\mathbf{n}_{FE} \quad \forall \boldsymbol{v}\in\mathcal{P}^k(F)^2.$$

- Space :

$$\underline{X}^k_{\mathbf{grad},F} = \Big\{ \underline{q}_F = (q_F, (q_E)_{E\in\mathcal{E}_F}, (q_V)_{V\in\mathcal{V}_F}) \,: \\ q_F \in \mathcal{P}^{k-1}(F)\,,\ q_E \in \mathcal{P}^{k-1}(E)\,,\ q_V \in \mathbb{R} \Big\},$$

- Face gradient $\mathbf{G}^k_F : \underline{X}^k_{\mathbf{grad},F} \to \mathcal{P}^k(F)^2$ s.t.

$$\int_F (\mathbf{G}^k_F \underline{q}_F)\cdot\boldsymbol{v} = -\int_F q_F \,\mathrm{div}_F\, \boldsymbol{v} + \sum_{E\in\mathcal{E}_F} \omega_{FE} \int_E (\gamma^{k+1}_E \underline{q}_E)\boldsymbol{v}\cdot\mathbf{n}_{FE} \quad \forall \boldsymbol{v} \in \mathcal{P}^k(F)^2.$$

- Potential reconstruction $\gamma^{k+1}_F : \underline{X}^k_{\mathbf{grad},F} \to \mathcal{P}^{k+1}(F)$ s.t.

$$\int_F (\gamma^{k+1}_F \underline{q}_F)\,\mathrm{div}_F\, \boldsymbol{z} = -\int_F \mathbf{G}^k_F \underline{q}_F \cdot \boldsymbol{z} + \sum_{E\in\mathcal{E}_F} \omega_{FE} \int_F (\gamma^{k+1}_E \underline{q}_E)\boldsymbol{z}\cdot\mathbf{n}_{FE} \\ \forall \boldsymbol{z} \in \boldsymbol{\mathcal{R}}^{\mathrm{c},k+2}(F) := (\boldsymbol{x}-\boldsymbol{x}_F)\mathcal{P}^{k+1}(F).$$

($\mathrm{div}_F : \boldsymbol{\mathcal{R}}^{\mathrm{c},k+2}(F) \to \mathcal{P}^{k+1}(F)$ *is an isomorphism*.)

Same principle! Based on IBP we determine:

- An additional unknown ($q_T \in \mathcal{P}^{k-1}(T)$) to get the space $\underline{X}^k_{\mathbf{grad},T}$, and its meaning (polynomial moment on T) to get the interpolator $\underline{I}^k_{\mathbf{grad},T}$.
- A formula for the element gradient $\mathbf{G}^k_T : \underline{X}^k_{\mathbf{grad},T} \to \mathcal{P}^k(T)^3$.
- A potential reconstruction $P^{k+1}_{\mathbf{grad},T} : \underline{X}^k_{\mathbf{grad},T} \to \mathcal{P}^{k+1}(T)$.

The Discrete de Rham method I

- Contrary to FE, do not seek explicit (or any!) basis functions.
- Fully discrete spaces made of vectors of polynomials, representing polynomial moments when interpreted through the interpolator.
- Polynomials attached to geometric entities to emulate expected continuity properties of each space,
- Create discrete operators (differential, potential reconstruction) between the spaces.

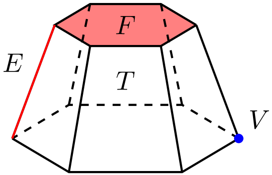

The Discrete de Rham method II

DDR complex:

$$\mathbb{R} \xrightarrow{\underline{I}^k_{\mathbf{grad},h}} \underline{X}^k_{\mathbf{grad},h} \xrightarrow{\underline{\boldsymbol{G}}^k_h} \underline{\boldsymbol{X}}^k_{\mathbf{curl},h} \xrightarrow{\underline{\boldsymbol{C}}^k_h} \underline{\boldsymbol{X}}^k_{\mathrm{div},h} \xrightarrow{D^k_h} \mathcal{P}^k(\mathcal{T}_h) \xrightarrow{0} \{0\}.$$

- Reproduces key properties of the continuous de Rham complex:
  - Same cohomology [Di Pietro et al., 2023] *(exact complex if trivial topology.)*
  - Uniform Poincaré inequalities [Di Pietro and Droniou, 2021a, Di Pietro and Droniou, 2023a, Di Pietro and Hanot, 2024b].
- Analytical properties [Di Pietro et al., 2023]:
  - Primal consistency: approximation properties of potential reconstructions, discrete operators and inner products
  - Adjoint consistency: estimate the error in discrete integration-by-parts involving the discrete operators.

The Discrete de Rham method III

L^2-like inner products: for $\bullet \in \{\mathbf{grad}, \mathbf{curl}, \mathrm{div}\}$, on $\underline{X}^k_{\bullet,h}$,

$$(\underline{\boldsymbol{v}}_h, \underline{\boldsymbol{w}}_h)_{\bullet,h} := \sum_{T\in\mathcal{T}_h} (\underline{\boldsymbol{v}}_h, \underline{\boldsymbol{w}}_h)_{\bullet,T}$$

$$\text{with } (\underline{\boldsymbol{v}}_h, \underline{\boldsymbol{w}}_h)_{\bullet,T} = \int_T \boldsymbol{P}^k_{\bullet,h}\underline{\boldsymbol{v}}_h \cdot \boldsymbol{P}^k_{\bullet,h}\underline{\boldsymbol{w}}_h + \mathrm{s}_{\bullet,T}(\underline{\boldsymbol{v}}_h, \underline{\boldsymbol{w}}_h),$$

where $\mathrm{s}_{\bullet,T}$ penalises differences on the boundary between element and face/edge potentials on T.

DDR scheme: replace continuous spaces/operators/L^2-products with discrete space/operators/L^2-like inner products.

Open-source C++ implementation available in HArDCore (https://github.com/jdroniou/HArDCore).

Outline

1. Some PDE models of interest
   - Stokes I
   - Stokes II
   - Navier–Stokes
   - Magnetostatics
2. De Rham complex
3. Discrete De Rham (DDR) complex
4. Applications to the models of interest

Slides

Stokes equations in curl-curl formulation: theorem

Theorem (Error estimates [Beirão da Veiga et al., 2022])

With the discrete $\boldsymbol{H}(\mathbf{curl})$*-like and* H^1*-like norms*

$$\|\underline{\boldsymbol{v}}_h\|^2_{\mathbf{curl},1,h} = \|\underline{\boldsymbol{v}}_h\|^2_{\mathbf{curl},h} + \|\underline{\boldsymbol{C}}_h^k \underline{\boldsymbol{v}}_h\|^2_{\mathrm{div},h}\,,$$
$$\|\underline{q}_h\|^2_{\mathbf{grad},1,h} = \|\underline{q}_h\|^2_{\mathbf{grad},h} + \|\underline{\boldsymbol{G}}_h^k \underline{q}_h\|_{\mathbf{curl},h},$$

we have the pressure robust estimates

$$\|\underline{\boldsymbol{u}}_h - \underline{\boldsymbol{I}}^k_{\mathbf{curl},h}\boldsymbol{u}\|_{\mathbf{curl},1,h} + \|\underline{p}_h - \underline{I}^k_{\mathbf{grad},h}p\|_{\mathbf{grad},1,h} \lesssim C_1(\boldsymbol{u})h^{k+1}.$$

with $C_1(\boldsymbol{u})$ *depending* $\boldsymbol{u}$ *and some of its derivatives, but not* p*.*

Robustness comes from:

Commutation property $\underline{\boldsymbol{G}}_h^k(\underline{I}^k_{\mathbf{grad},h}p) = \underline{\boldsymbol{I}}^k_{\mathbf{curl},h}(\mathbf{grad}\,p)$.

Stokes equations in curl-curl formulation: tests I

- $\Omega = (0,1)^3$.
- Voronoi mesh families (similar results on tetrahedral meshes):

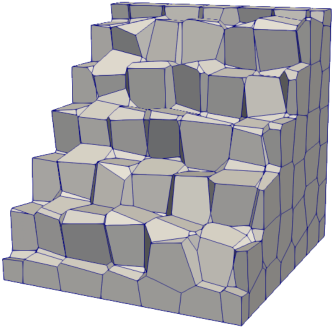

(a) Voronoi mesh

Stokes equations in curl-curl formulation: tests II

- Exact solution: for some $\lambda \geq 0$,

$$p(x,y,z) = \lambda \sin(2\pi x)\sin(2\pi y)\sin(2\pi z)\,,$$

$$\boldsymbol{u}(x,y,z) = \begin{bmatrix} \frac{1}{2}\sin(2\pi x)\cos(2\pi y)\cos(2\pi z) \\ \frac{1}{2}\cos(2\pi x)\sin(2\pi y)\cos(2\pi z) \\ -\cos(2\pi x)\cos(2\pi y)\sin(2\pi z) \end{bmatrix}.$$

- Measured errors:
  - E^{d} in discrete norms between the approximate solutions and the *interpolates* of the exact solution (as in the theorems).
  - E^{c} in continuous norms between reconstructed potentials of the approximate solutions and the exact solution.

Stokes equations in curl-curl formulation: tests III

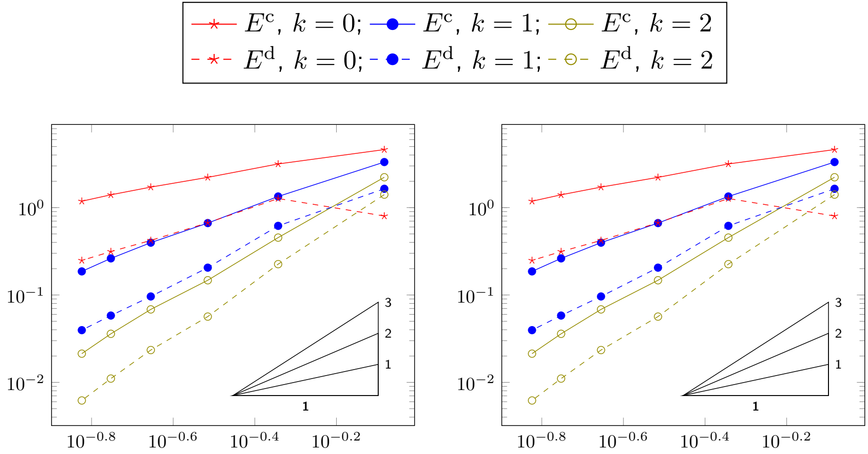

(a) Errors on $\boldsymbol{u}$, $\lambda = 1$

(b) Errors on $\boldsymbol{u}$, $\lambda = 1e5$

Stokes equations in curl-curl formulation: tests IV

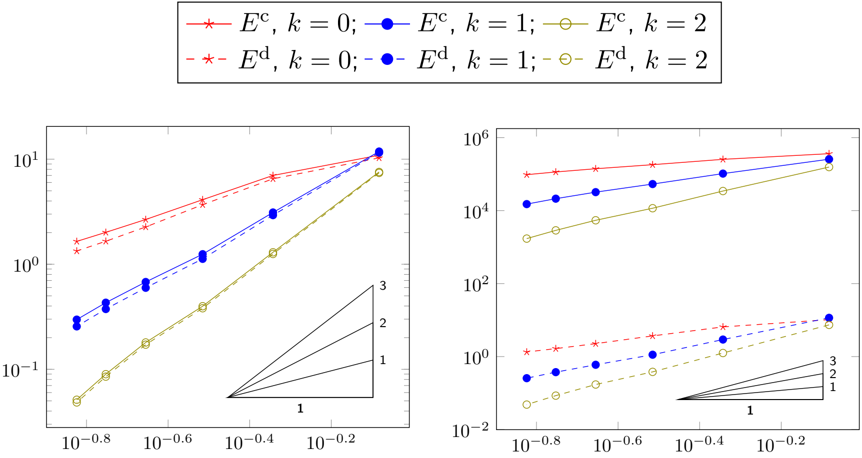

(a) Errors on $\mathbf{grad}\, p$, $\lambda = 1$

(b) Errors on $\mathbf{grad}\, p$, $\lambda = 1e5$

Navier–Stokes in curl-curl formulation: theorem

Theorem (Error estimates [Di Pietro et al., 2024])

Define the discrete L^4-Sobolev constant by

$$C_{\mathrm{S},h} := \max\left\{ \frac{\|\boldsymbol{P}^k_{\mathbf{curl},h}\underline{\boldsymbol{v}}_h\|_{\boldsymbol{L}^4(\Omega)}}{\|\underline{\boldsymbol{C}}^k_h\underline{\boldsymbol{v}}_h\|_{\mathrm{div},h}} \;:\; \underline{\boldsymbol{v}}_h \in (\operatorname{Im}\underline{\boldsymbol{G}}^k_h)^\perp \setminus \{\mathbf{0}\} \right\}.$$

With $\mathbf{R}_{\boldsymbol{u}}$ solenoidal part of forcing term $\boldsymbol{f}$ (depends only on $\boldsymbol{u}$), if

$$C^2_{\mathrm{S},h}\|\underline{\boldsymbol{I}}^k_{\mathbf{curl},h}(\mathbf{R}_{\boldsymbol{u}})\|_{\mathbf{curl},h} \text{ is small enough,}$$

then

$$\|\underline{\boldsymbol{u}}_h - \underline{\boldsymbol{I}}^k_{\mathbf{curl},h}\boldsymbol{u}\|_{\mathbf{curl},h} + \|\underline{\boldsymbol{C}}^k_h(\underline{\boldsymbol{u}}_h - \underline{\boldsymbol{I}}^k_{\mathbf{curl},h}\boldsymbol{u})\|_{\mathrm{div},h} \lesssim C(\boldsymbol{u})h^{k+1}.$$

- Robust estimate with respect to the pressure.
- Boundedness of $C_{S,h}$ w.r.t. h still an open question (expected for convex domains).

Navier–Stokes in curl-curl formulation: convergence tests I

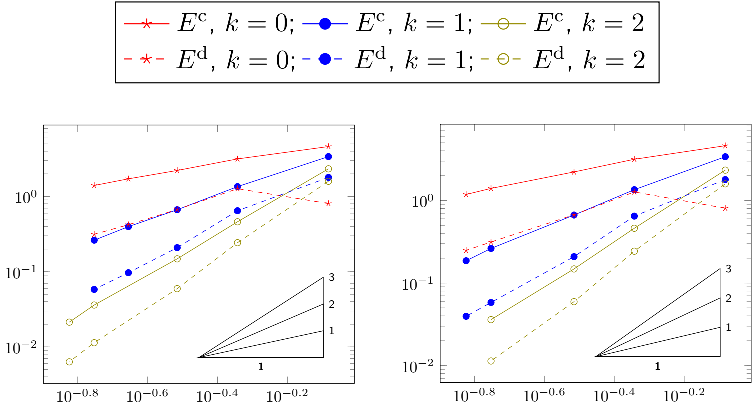

(a) Errors on $\boldsymbol{u}$, $\lambda = 1$

(b) Errors on $\boldsymbol{u}$, $\lambda = 10^2$

Navier–Stokes in curl-curl formulation: convergence tests II

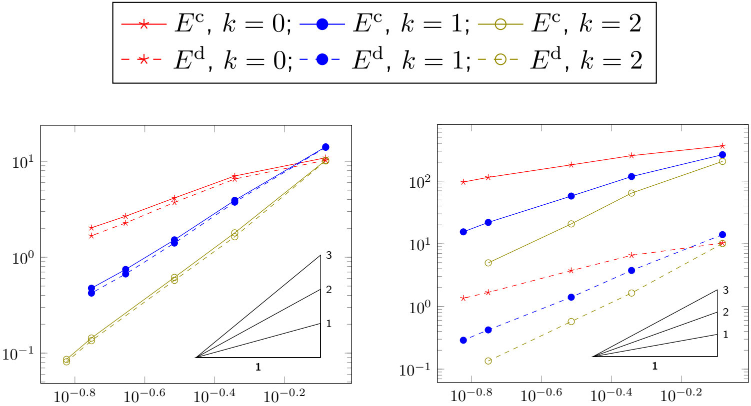

(a) Errors on $\mathbf{grad}\, p$, $\lambda = 1$

(b) Errors on $\mathbf{grad}\, p$, $\lambda = 10^2$

Navier–Stokes: flow in cavity with mixed BCs I

In the unit cube $\Omega = (0,1)^3$:

- Essential BCs (pressure and tangential velocity):

$$p(x,y,z) = -z \quad \text{and} \quad \boldsymbol{u} \times \mathbf{n} = \mathbf{0}$$

on the bottom corner $\{0\} \times (0, 0.25) \times (0, 0.25)$ of the face $x = 0$.

- Natural BCs (tangential vorticity and flux):

$$\mathbf{curl}\, \boldsymbol{u} \times \mathbf{n} = \mathbf{0} \quad \text{and} \quad \boldsymbol{u} \cdot \mathbf{n} = 1$$

on the bottom corner $\{1\} \times (0, 0.25) \times (0, 0.25)$ of the face $x = 1$,

- Homogeneous natural BCs elsewhere.

Navier–Stokes: flow in cavity with mixed BCs II

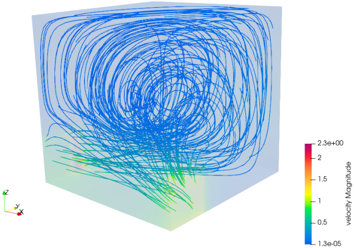

(a) Velocity

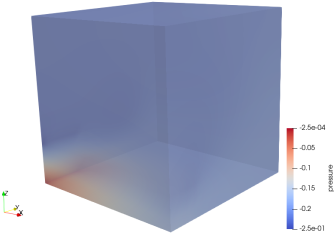

(b) Pressure

Figure: Velocity streamlines and pressure

Reissner–Mindlin

Model:

$$
\begin{aligned}
\boldsymbol{\gamma} + \operatorname{div}(\boldsymbol{C}\,\mathbf{grad}_s\,\boldsymbol{\theta}) &= \mathbf{0} && \text{in } \Omega,\\
-\operatorname{div}\boldsymbol{\gamma} &= f && \text{in } \Omega,\\
\boldsymbol{\gamma} &= \frac{\kappa}{t^2}(\mathbf{grad}\,u - \boldsymbol{\theta}) && \text{in } \Omega,\\
\boldsymbol{\theta} = \mathbf{0}, \quad u &= 0 && \text{on } \partial\Omega.
\end{aligned}
$$

- Ω polygonal domain (2D), t: plate thickness.
- $\boldsymbol{\gamma}$: shear strain; $\boldsymbol{\theta}$: fibers rotations; u: transverse displacement.
- f: transverse load; $\boldsymbol{C}$: linear elasticity tensor; κ: shear modulus.

Reissner–Mindlin

Model:

$$\begin{aligned} \boldsymbol{\gamma} + \operatorname{div}(\boldsymbol{C}\,\mathbf{grad}_s\,\boldsymbol{\theta}) &= \mathbf{0} && \text{in } \Omega,\\ -\operatorname{div}\boldsymbol{\gamma} &= f && \text{in } \Omega,\\ \boldsymbol{\gamma} &= \frac{\kappa}{t^2}(\mathbf{grad}\,u - \boldsymbol{\theta}) && \text{in } \Omega,\\ \boldsymbol{\theta} = \mathbf{0},\quad u &= 0 && \text{on } \partial\Omega. \end{aligned}$$

- Ω polygonal domain (2D), t: plate thickness.
- $\boldsymbol{\gamma}$: shear strain; $\boldsymbol{\theta}$: fibers rotations; u: transverse displacement.
- f: transverse load; $\boldsymbol{C}$: linear elasticity tensor; κ: shear modulus.

Scheme: [Di Pietro and Droniou, 2021b].

- Approximation space for u: $\underline{X}^k_{\mathbf{grad},h}$.
- Approximation space for $\boldsymbol{\theta}$: $\underline{\boldsymbol{X}}^k_{\mathbf{curl},h}$ enriched with full vector-valued polynomials on the edges (not just tangential components).

Reissner–Mindlin: theorems I

Theorem (Error estimate for arbitrary k)

If the solution $(\boldsymbol{\eta}, u)$ *satisfies* $u \in C^1(\overline{\Omega}) \cap H^{k+2}(\Omega)$ *and* $\boldsymbol{\theta} \in H^1(\Omega)^2 \cap H^{k+2}(\Omega)^2$, *then*

$$\|(\underline{\boldsymbol{\theta}}_h - \underline{I}_{\boldsymbol{\Theta},h}\boldsymbol{\theta}, \underline{u}_h - \underline{I}_{\mathbf{grad},h}u)\|_{L^2} \lesssim h^{k+1}\left(|\boldsymbol{\theta}|_{H^{k+2}} + |\boldsymbol{\gamma}|_{H^{k+1}}\right).$$

- Optimal rate of convergence, but not robust w.r.t. $t \to 0$ (even for $k = 0$).
- Lack of robustness for $k \geq 1$ observed on solutions s.t. $|\boldsymbol{\gamma}|_{H^{k+1}} \sim t^{-k-\frac{1}{2}}$.

Reissner–Mindlin: theorems II

Theorem (Locking-free error estimate for $k = 0$)

Under the previous assumptions and $k = 0$, it holds

$$\|(\underline{\boldsymbol{\theta}}_h - \underline{\boldsymbol{I}}_{\boldsymbol{\Theta},h}\boldsymbol{\theta}, \underline{u}_h - \underline{I}_{\mathbf{grad},h}u)\|_{L^2} \lesssim h\left(|\boldsymbol{\theta}|_{H^2} + t|\boldsymbol{\gamma}|_{H^1} + \|\boldsymbol{\gamma}\|_{L^2} + \|f\|_{L^2}\right).$$

- Fully robust w.r.t. t: $|\boldsymbol{\theta}|_{H^2} + t|\boldsymbol{\gamma}|_{H^1} + \|\boldsymbol{\gamma}\|_{L^2} + \|f\|_{L^2} \lesssim 1$.
  $\rightsquigarrow$ Observed in numerical tests.
- Proof relies on:
  - Commutation property $\underline{\boldsymbol{G}}_h^k(\underline{I}_{\mathbf{grad},h}^k u) = \underline{\boldsymbol{I}}_{\mathbf{curl},h}^k(\mathbf{grad}\, u)$,
  - Conforming lifting of U_h, and a piecewise-constant lifting on $\boldsymbol{\Theta}_h$ based on a local discrete Hodge decomposition.

  Both challenging because of the polygonal mesh...

Reissner–Mindlin: test

Stabilised $\mathcal{P}_2$-($\mathcal{P}_1 + \mathcal{B}^3$) scheme		DDR scheme	
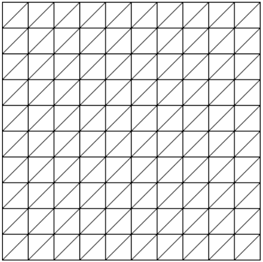		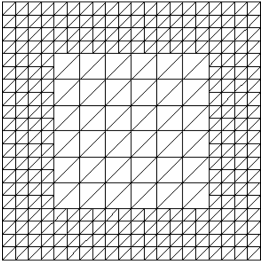	
nb. DOFs	Error	nb. DOFs	Error
2403	0.138	550	0.161
9603	6.82e-2	2121	6.77e-2
38402	3.40e-2	8329	3.1e-2

Conclusions and extensions I

- Discrete version of the de Rham complex, of arbitrary degree of accuracy and applicable to polytopal meshes.
  Other discrete polytopal complex based on VEM [Beirão da Veiga et al., 2018], see connexions in [Beirão da Veiga et al., 2022].

- Full theory:
  - Algebraic properties: same cohomology as the continuous de Rham complex on any domain, commutation properties between interpolants and discrete operators, etc.
  - Analytic properties: Poincaré inequalities, primal and adjoint consistency, etc.

- Polytopal exterior calculus version: complex written in the framework of differential forms (see Finite Element Exterior Calculus for FE methods). [Bonaldi et al., 2024].

- DDR on manifolds, with application to Maxwell [Droniou et al., 2024].

Conclusions and extensions II

- Other polytopal complexes based on DDR approach (see Marwa Salah's presentation to follow): plate complexes, divdiv complexes (2D and 3D), Stokes complex...
- Applications:
  - Magnetostatics. [Di Pietro and Droniou, 2021a]
  - Stokes equations in standard form. [Hanot, 2023]
  - Kirchoff plate. [Di Pietro and Droniou, 2023b]
  - Quad-rot problem. [Di Pietro, 2024]
  - Biharmonic problems. [Di Pietro and Hanot, 2024a]

- Notes and series of introductory lectures to DDR:

  https://math.unice.fr/~massonr/Cours-DDR/Cours-DDR.html

COURSE OF JEROME DRONIOU FROM MONASH UNIVERSITY, INVITED PROFESSOR AT UCA

- **Introduction to Discrete De Rham complexes**
  - Short description (in french)
  - Summary of notations and formulas
  - Part 1, first course: the de Rham complex and its usefulness in PDEs, 22/09/22 (video)
  - Part 1, second course: Low order case, 29/09/22 (video)
  - Part 1, third course: Design of the DDR complex in 2D, 07/10/22 (video)
  - Part 1, fourth course: Exactness of the DDR complex in 2D, 10/10/22 (video)
  - Part 2, fifth course: DDR in 3D, analysis tools, 17/11/22 (video)

Funded by the European Union (ERC Synergy, NEMESIS, project number 101115663). Views and opinions expressed are however those of the authors only and do not necessarily reflect those of the European Union or the European Research Council Executive Agency. Neither the European Union nor the granting authority can be held responsible for them.

Thank you for your attention!

References I

Arnold, D. (2018).
Finite Element Exterior Calculus.
SIAM.

Beirão da Veiga, L., Brezzi, F., Dassi, F., Marini, L. D., and Russo, A. (2018).
A family of three-dimensional virtual elements with applications to magnetostatics.
SIAM J. Numer. Anal., 56(5):2940–2962.

Beirão da Veiga, L., Dassi, F., Di Pietro, D. A., and Droniou, J. (2022).
Arbitrary-order pressure-robust ddr and vem methods for the stokes problem on polyhedral meshes.
Comput. Methods Appl. Mech. Engrg., 397:Paper No. 115061.

Bonaldi, F., Di Pietro, D. A., Droniou, J., and Hu, K. (2024).
An exterior calculus framework for polytopal methods.
Journal of the European Mathematical Society, page 55p.

Di Pietro, D. A. (2024).
An arbitrary-order discrete rot-rot complex on polygonal meshes with application to a quad-rot problem.
IMA J. Numer. Anal., 44(3):1699–1730.

Di Pietro, D. A. and Droniou, J. (2020).
The Hybrid High-Order method for polytopal meshes.
Number 19 in Modeling, Simulation and Application. Springer International Publishing.

References II

Di Pietro, D. A. and Droniou, J. (2021a).
An arbitrary-order method for magnetostatics on polyhedral meshes based on a discrete de Rham sequence.
J. Comput. Phys., 429(109991).

Di Pietro, D. A. and Droniou, J. (2021b).
A DDR method for the Reissner–Mindlin plate bending problem on polygonal meshes.

Di Pietro, D. A. and Droniou, J. (2023a).
An arbitrary-order discrete de Rham complex on polyhedral meshes: Exactness, Poincaré inequalities, and consistency.
Found. Comput. Math., 23:85–164.

Di Pietro, D. A. and Droniou, J. (2023b).
A fully discrete plates complex on polygonal meshes with application to the Kirchhoff–Love problem.
Math. Comp., 92(339):51–77.

Di Pietro, D. A. and Droniou, J. (2023c).
Homological- and analytical-preserving serendipity framework for polytopal complexes, with application to the DDR method.
ESAIM: Math. Model Numer. Anal., 57(1):191–225.

Di Pietro, D. A., Droniou, J., and Pitassi, S. (2023).
Cohomology of the discrete de Rham complex on domains of general topology.
Calcolo.
Published online.

Di Pietro, D. A., Droniou, J., and Qian, J. J. (2024).
A pressure-robust Discrete de Rham scheme for the Navier-Stokes equations.
Comput. Methods Appl. Mech. Engrg., 421:Paper no. 116765, 21p.

Di Pietro, D. A., Droniou, J., and Rapetti, F. (2020).
Fully discrete polynomial de Rham sequences of arbitrary degree on polygons and polyhedra.
Math. Models Methods Appl. Sci., 30(9):1809–1855.

Di Pietro, D. A. and Hanot, M.-L. (2024a).
A discrete three-dimensional divdiv complex on polyhedral meshes with application to a mixed formulation of the biharmonic problem.
Math. Models Methods Appl. Sci., 34(9):1597–1648.

Di Pietro, D. A. and Hanot, M.-L. (2024b).
Uniform poincaré inequalities for the discrete de rham complex on general domains.
Results Appl. Math., 23(100496).

Droniou, J., Hanot, M., and Oliynyk, T. (2024).
A polytopal discrete de rham complex on manifolds, with application to the maxwell equations.
page 33p.

References IV

Hanot, M.-L. (2023).
An arbitrary-order fully discrete Stokes complex on general polyhedral meshes.
Math. Comp., 92(343):1977–2023.